

# Charge transfer and polarization screening in organic thin films: phthalocyanines on Au(100)

Daniel Kolacyak · Heiko Peisert · Thomas Chassé

Received: 19 June 2008 / Accepted: 24 November 2008 / Published online: 16 December 2008  
© Springer-Verlag 2008

**Abstract** Core hole screening effects at organic/metal interfaces were studied by core level X-ray photoemission spectroscopy (XPS), X-ray excited Auger electron spectroscopy (XAES), and valence band ultraviolet photoemission spectroscopy (UPS). The comparison of energetic shifts in XPS and XAES enables the estimation of electronic relaxation energy (screening ability). Magnesium phthalocyanine (MgPc) and zinc phthalocyanine (ZnPc) evaporated on single crystalline Au(100) were used as model molecules. Two different features in the Mg KLL spectra can be clearly separated for (sub-)monolayer coverages, while only minor changes of the shape of Mg 1s are observed. Applying a dielectric continuum model, the major screening mechanism cannot be described sufficiently by polarization screening due to mirror charges, significant contributions by charge transfer screening have to be considered. In contrast, small screening effects in the bulk material can be explained by surface polarization.

**PACS** 72.80.Le · 79.60.Fr · 73.20.-r

## 1 Introduction

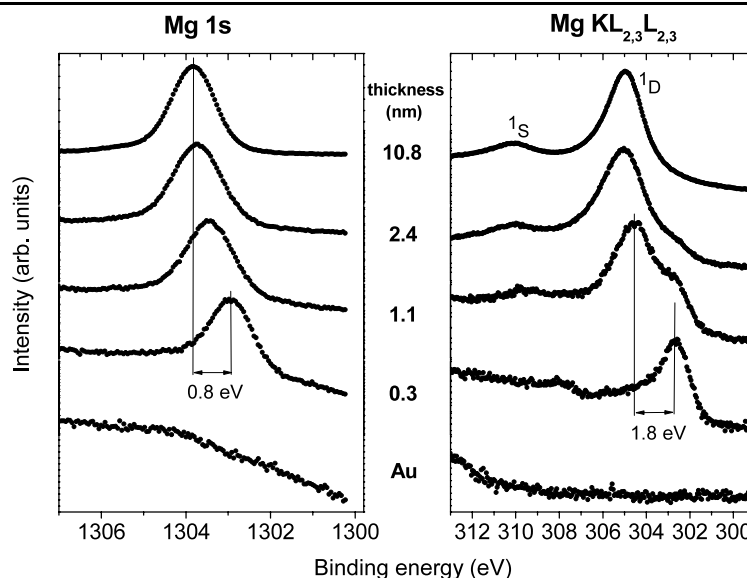
In bulk organic materials charges are screened by the environment. In particular, the electronic polarization of the dielectric medium affects significantly the charge carrier transport. The transport gap  $E_t$ , i.e., the energy difference between the transport levels for holes and electrons, has a substantial polarization energy contribution [1–3]. In addition,

at surfaces and interfaces the electronic polarization is different compared to the bulk organic material [2, 3], which may affect the charge carrier injection [4, 5].

We focus in this work on core hole screening effects in organic materials as well as at organic/metal interfaces using combined photoemission spectroscopy (PES) and X-ray excited Auger electron spectroscopy (XAES). Results from X-ray photoemission spectroscopy (XPS) and valence band ultraviolet photoemission spectroscopy (UPS) are compared. In photoemission spectroscopy, the screening of the photo-hole is described within the initial state—final state framework by the dynamical or one-hole relaxation energy  $R_D$ . Due to the different final states in PES (one hole) and XAES (two holes),  $R_D$  is about threefold higher in the case of Auger spectra. Thus,  $\Delta R_D$  may be semi-quantitatively derived by the comparison of binding energy ( $E_B$ ) shifts in XPS and XAES via the modified Auger parameter  $\alpha'$ :  $\Delta\alpha' = \Delta E_B(\text{XPS}) - \Delta E_B(\text{XAES})$ . The Auger parameter shift contains contributions from intra-atomic screening, relaxation by charge transfer and environment screening [6]. It can be shown that  $D\alpha'$  correlates well with the change of the electronic polarization energy for the core hole ( $\Delta\alpha' \cong 2\Delta R_D$ ) [7]. Furthermore,  $\Delta R_D$  can be correlated with the change of the polarization energy induced by the redistribution of environmental charges presuming similar intra-molecular screening and excluding extra-molecular charge transfer within the time scale of the photoemission. Although  $R_D$  is larger for core holes compared to valence holes, changes of these terms are comparable in a good approximation and correlate with frequently discussed changes of the electronic (valence) polarization energy ( $\Delta E_P$  or  $\Delta P_+$ ). It was shown that screening does not only affect the measured absolute core level  $E_B$  in solids but also the measured  $E_B$  at interfaces [8–11].

D. Kolacyak · H. Peisert (✉) · T. Chassé  
Institute of Physical and Theoretical Chemistry, University of  
Tübingen, Auf der Morgenstelle 8, 72076 Tübingen, Germany  
e-mail: heiko.peisert@uni-tuebingen.de  
Fax: +49-7071-295490

**Fig. 1** MgPc/Au(100): Mg 1s photoemission spectra (*left*) and Mg KLL Auger spectra (*right*) of incrementally deposited MgPc on single crystalline Au(100). Visible Auger transitions ( $^1D$ ,  $^1S$ ) are denoted. The well resolved additional feature at the earliest stages of deposition appears only in the Auger spectra



As a model molecule we chose magnesium phthalocyanine (MgPc), evaporated onto Au(100), a system where no chemical interaction occurs. The results are compared to recently studied MgPc on polycrystalline gold [11]. For the analysis of differences in the screening between bulk and surface, MgPc was embedded as a probe molecule in a zinc phthalocyanine (ZnPc) matrix.

## 2 Experimental

The measurements were performed using a multi-chamber UHV-system (base pressure  $2 \times 10^{-10}$  mbar), equipped with a Phoibos 100 cylindrical hemispherical analyzer (SPECS), a monochromatic Al  $K\alpha$  source and a He discharge lamp. The energetic resolution determined from the width of the Fermi edge for XPS and UPS was about 400 meV and 100 meV, respectively. Organic films were evaporated in a step-wise manner, the pressure during the evaporation was less than  $5 \times 10^{-8}$  mbar and the evaporation rate was about  $0.1 \text{ \AA/s}$ . The film thickness was controlled by a quartz microbalance calibrated using the attenuation of XPS intensities during the initial deposition steps. Due to careful comparison of single scans possible radiation damages can be excluded, several series of spectra with different radiation exposure times were taken.

The Au(100) single crystal has been cleaned by cycles of sputtering and annealing. The cleanliness of the gold surface was checked using core level X-ray photoemission spectroscopy (XPS) and low-energy electron-diffraction (LEED), no sign of contamination could be detected and a sharp LEED pattern ( $5 \times 20$  superstructure) was obtained.

## 3 Results and discussion

In Fig. 1, we compare Mg 1s photoemission core level spectra and Mg  $KL_{2,3}L_{2,3}$ ,  $^1D$  Auger spectra of incrementally deposited films of MgPc on single crystalline Au(100). In both cases, a strong shift of spectral features to higher binding energies ( $E_{BS}$ ) with increasing film thickness can be observed. Such strong energetic shifts within the first nanometers of the organic film (typically about 2 nm) are a result of the formation of interface dipoles. The mechanism of the dipole formation was discussed intensively in the past years by various groups [5, 10, 12–19]. Several contributions have been proposed, including the polarization effects. Most importantly in Fig. 1, we observe for ultrathin films in the monolayer range (0.3 and 1.1 nm film thickness) two clearly separated different features in the Mg KLL Auger spectra, while only minor changes of the shape of Mg 1s photoemission spectra are observed. The separation of the two Auger signals is as large as 1.8 eV. From the analysis of the Auger peak ratio at 1.1 nm (Fig. 1) we conclude that the difference of the screening is mainly related to the first molecular layer at the interface (assuming analogously to CuPc lying molecules [20] and a molecule–molecule distance of about 0.34 nm [21]).

The same behavior was recently also observed for MgPc on polycrystalline Au [11]. On polycrystalline gold the orientation of the related phthalocyanines changes during the growth: within the first 2–4 layers the molecules are lying on the substrate surface, whereas a preferred standing orientation is usually observed at higher coverages [22, 23]. The orientation and packing in thin organic films, however, may affect electronic properties such as the ionization potential considerably, as recently shown, e.g., for sexiphenyl and dihexylsexithiophene [24, 25].

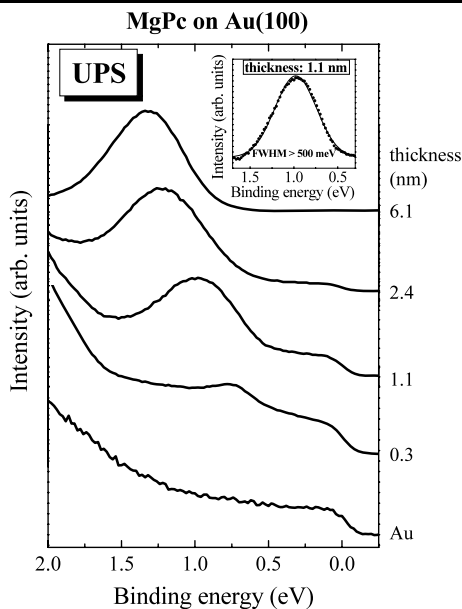


**Fig. 2** Valence band photoemission spectra of incrementally deposited MgPc on Au(100). Similar to the core level photoemission spectra of Fig. 1, no clearly separated additional features for low coverages can be observed. *Inset:* The detailed analysis of the HOMO at 1.1 nm by a peak fitting routine yields to FWHM > 500 meV

Our results on Au(100) indicate that a change of the molecular orientation is not responsible for the observed change of the Auger peak energy directly at the interface to gold.

Since  $\Delta R_D$  is about threefold higher for Auger spectra (see above) compared to photoemission spectra, the appearance of the splitting of the Auger signal only may suggest an attribution predominantly to final state screening effects. In the case of polarization screening, we would expect a splitting of the Mg 1s photoemission spectra by about 0.6 eV, which may not be energetically resolved. The better energetic resolution in valence band photoemission spectroscopy (UPS) and the usually sharp valence band structures enable even the separation of photoemission features with small energetic distances. UPS spectra for MgPc on Au(100) as a function of the layer thickness are shown in Fig. 2 (zoom into the highest occupied molecular orbital, HOMO). Similar to the core level photoemission spectra of Fig. 1, no additional features for low coverages are visible, analogously to published data of related systems [10]. On the other hand, a slight broadening might be observed at a film thickness of about 1.1 nm, the detailed analysis of the HOMO by a peak fitting routine [26], applying a polynomial background and a Voigt profile peak shape, results in a full width at half maximum (FWHM) of about 550 meV (inset of Fig. 2). Presuming two components with the same shape the peak fit, however, yields to an upper limit for a possible splitting of 0.3 eV, significantly lower than 0.6 eV (not shown). This

**Table 1** Layer dependent screening contributions estimated by dielectric continuum model. For the distance of the first layer to the mirror plane of the metal, we apply the van der Waals radius of carbon in organic compounds (0.17 nm, *middle*). For comparison, we also chose a significantly smaller (0.15 nm, *left*) and larger (0.20 nm, *right*) value

	$d$	$\Delta R_D$	$d$	$\Delta R_D$	$d$	$\Delta R_D$
	(nm)	(eV)	(nm)	(eV)	(nm)	(eV)
1st layer	0.15	0.80	0.17	0.71	0.20	0.60
2nd layer	0.49	0.25	0.51	0.24	0.54	0.22
3rd layer	0.83	0.15	0.85	0.14	0.88	0.14

points to underlying reasons other than polarization screening for the observed phenomena.

The question now arises whether or not the order of magnitude of the energetic shifts in the Auger spectra of MgPc on Au(100) could be understood by polarization screening. The electronic polarization energy  $\Delta R_D$  for the core hole can be determined experimentally via the Auger parameter (see above). In Fig. 3, we compare the modified Auger parameter  $\alpha' = E_{\text{kin}}(\text{Mg KL}_{2,3}\text{L}_{2,3}, {}^1\text{D}) + E_B(\text{Mg } 1\text{ s})$  (here  $E_{\text{kin}}$  denotes the kinetic energy of the Auger transition) for MgPc/Au(100) (left) to MgPc/polycrystalline Au (right). In both cases, we distinguish clearly between interface and bulk signals; the distance  $\Delta\alpha'$  is about 1.8 eV. Thus, the estimation of the relaxation energy  $R_D$  for molecules directly at the metal surface and molecules in thicker films via the Auger parameter yields a difference  $\Delta R_D \sim 0.9$  eV. We note that a possible separation of the photoemission signals into bulk and interface is not considered (see above, maximal possible splitting of the HOMO signal by 0.3 eV), in this case  $\Delta\alpha'$  may be lowered by 0.3 eV.

Otherwise, layer dependent screening contributions due to polarization screening can be estimated applying a dielectric continuum model. For metal–dielectric interfaces we calculate  $\Delta E_B$  according to  $\Delta E_B(d) - \Delta E_B(\infty) = -e^2/(16\pi\epsilon_0\epsilon \cdot d)$  [8, 9, 11], where  $d$  is the distance from the mirror plane,  $\Delta E_B(d)$  and  $\Delta E_B(\infty)$  are referred to the distance  $d$  and the infinitely thick film, respectively. The dielectric constant  $\epsilon$  is assumed to be about 3, and for the molecule–molecule distance we apply the bulk value of 0.34 nm [21]. The distance of the first layer to the mirror plane of the metal  $d_1$  could be different on a microscopic scale, for instance, due to a distortion of molecules which was recently reported for CuPcF<sub>16</sub> on metal single crystals [27]. Analogously to [9], we apply the van der Waals radius of the adsorbate; for carbon in organic compounds  $d_1$  is about 0.17 nm. This model is schematically drawn in Fig. 4. The results of the calculation, compared with a distinct larger and smaller value for  $d_1$  (0.20 and 0.15 nm, respectively), are summarized in Table 1. The difference of  $\Delta R_D$  between the first and the second layer does not depend much on  $d_1$ , for  $d_1 = 0.17$  nm, 0.20 nm and 0.15 nm,

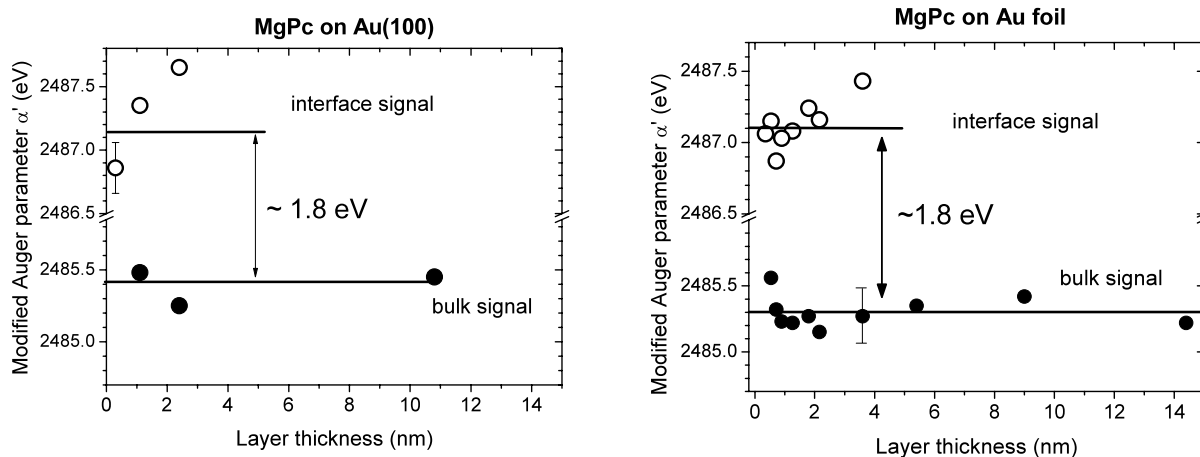


**Fig. 3** Comparison of modified Auger parameters  $\Delta\alpha' = \Delta E_B(\text{XPS}) - \Delta E_B(\text{XAES})$  for MgPc on Au foil and on Au(100). The average difference  $\Delta\alpha'$  for the interface and the bulk signal (1.8 eV) is similar in both cases

the values are significantly lower ( $\Delta R_D \sim 0.47$  eV, 0.38 eV, and 0.55 eV, respectively) as compared to the experimental observations. In order to explain the experimental  $\Delta R_D$  of about 0.9 eV, a distance of the first layer to the mirror plane much smaller than the van der Waals radius has to be assumed, which is not reasonable. Thus, the observed splitting in the Auger signals could be understood only partly by polarization screening. Therefore, we suggest a charge transfer within the time scale of the Auger transition as a possible screening mechanism. As recently experimentally observed [28], charge transfer processes at organic interfaces may occur in a femtosecond time scale, i.e., faster than the photoemission process in that case. The final state charge transfer may be promoted by hybridization between molecular states and metal states in the initial state [29] and/or by induced interface states [18]. Since an electron transfer to the molecule is the most effective screening mechanism, large energetic shifts in the Auger spectra can be expected.

Also visible from Fig. 3 is a distinct increase of  $\alpha'$  for the interface with growing film thickness. A possible reason for an increasing polarization energy and thus for a higher  $\alpha'$  could be a rise in the polarization ability of the environment of the molecules under consideration. Comparing molecules at the organic–vacuum interface to buried molecules, the photoemission final state can be better screened in the latter case since the vacuum is not polarizable. In other words, the polarization of layers above the considered molecule can contribute to the screening of the photohole.

In order to study the size of the “surface polarization” more in detail, we performed a supplementary experiment: MgPc was embedded in a ZnPc matrix and the change of the Auger parameter of Mg in MgPc was observed. Initially a 2.5 nm thick ZnPc film was evaporated on Au(100), followed by a probe (mono-)layer of MgPc (0.3 nm), and finally ZnPc was evaporated sequentially on top up to a total

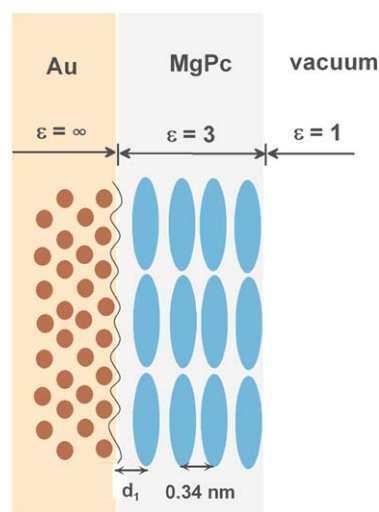


**Fig. 4** Scheme for the estimation of the polarization screening using a macroscopic dielectric model

organic film thickness of 4.8 nm. The initial film thickness of 2.5 nm ensures a negligible screening contribution due to the metal substrate on the probe layer. The modified Auger parameters for both ZnPc ( $\alpha' = E_{\text{kin}}(\text{ZnL}_3\text{M}_{4,5}\text{L}_{4,5}, {}^1\text{G}) + E_B(\text{Zn } 2p_{3/2})$ ) and MgPc as a function of the total organic film thickness are shown in Fig. 5. Whereas  $\alpha'$  for ZnPc stays nearly constant during the film growth, probably due to the overlapping of signals from different thicknesses, small but distinct changes for MgPc are identifiable. The modified Auger parameter  $\alpha'$  (MgPc) increases by 0.17 eV due to the polarization of ZnPc molecules evaporated on the MgPc probe layer. Thus, small changes in the Auger parameter can be attributed to surface polarization, but the resulting change of the polarization energy ( $\sim 0.5 \cdot \Delta\alpha'$ , see above) here is 0.1 eV or smaller, in good agreement with previous results [3, 25, 30]. We ascribe the observed larger changes of

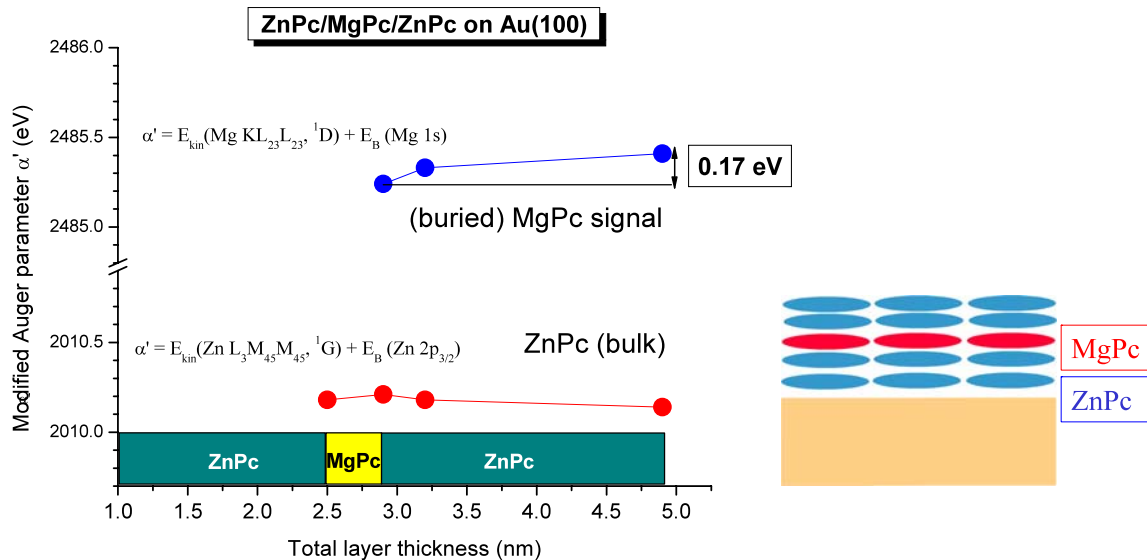


**Fig. 5** (color) Modified Auger parameter  $\alpha'$  for MgPc embedded in a ZnPc matrix (substrate: Au(100)). Small changes of  $\alpha'$  can be caused by additional polarization screening of ZnPc molecules above the MgPc probe layer

the (interface) Auger parameter in Fig. 3 to the different information depth of the analyzed signals: The photoemission signal contains information from several layers with most intensity from the sample surface, whereas the Auger signal arises from the interface.

In summary, we have shown that combined photoemission spectroscopy and X-ray excited Auger electron spectroscopy can be used as a tool to study the screening mechanism of holes at organic interfaces. From the comparison of energy shifts for Auger and photoemission spectra as well as from the estimation of layer resolved energy shifts applying a dielectric continuum model we conclude that the screening mechanism of the double hole final state of the Mg  $\text{KL}_{2,3}\text{L}_{2,3}, {}^1\text{D}$  transition for the first molecular MgPc layer on Au(100) cannot be described sufficiently by polarization screening due to mirror charges, significant contributions by charge transfer screening have to be considered. Using MgPc as a probe molecule in a ZnPc environment, the surface polarization energy for this system was estimated to be about 0.1 eV.

**Acknowledgements** We are grateful to W. Neu and I. Biswas for valuable discussions and technical support. The work was supported by the German Research Council Ch 132/20-1.

## References

- I.G. Hill, A. Kahn, Z.G. Soos, R.A. Pascal Jr., Chem. Phys. Lett. **327**, 181 (2000)
- E.V. Tsiper, Z.G. Soos, W. Gao, A. Kahn, Chem. Phys. Lett. **360**, 47 (2002)
- E.V. Tsiper, Z.G. Soos, Phys. Rev. B **68**, 085301 (2003)
- X.-Y. Zhu, Surf. Sci. Rep. **56**, 1 (2004)
- N. Koch, A. Vollmer, S. Duhm, Y. Sakamoto, T. Suzuki, Adv. Mater. **19**, 112 (2007)
- T.D. Thomas, P. Weightman, Phys. Rev. B **33**, 5406 (1986)
- H. Peisert, T. Chassé, P. Streubel, A. Meisel, R. Szargan, J. Electron Spectrosc. Relat. Phenom. **68**, 321 (1994)
- G. Kaindl, T.-C. Chiang, D.E. Eastman, F.J. Himpsel, Phys. Rev. Lett. **45**, 1808 (1980)
- T.-C. Chiang, G. Kaindl, G. Mandel, Phys. Rev. B **33**, 695 (1986)
- H. Peisert, T. Schwieger, J.M. Auerhammer, M. Knupfer, M.S. Golden, J. Fink, J. Appl. Phys. **91**, 4872 (2002)
- H. Peisert, A. Petershans, T. Chassé, J. Phys. Chem. C **112**, 5703 (2008)
- H. Ishii, K. Sugiyama, E. Ito, K. Seki, Adv. Mater. **11**, 605 (1999)
- X. Crispin, V. Geskin, A. Crispin, J. Cornil, R. Lazzaroni, W.R. Salaneck, J.L. Brédas, J. Am. Chem. Soc. **124**, 8131 (2002)
- J. Campbell Scott, J. Vac. Sci. Technol. A **21**, 521 (2003)
- M. Knupfer, H. Peisert, Phys. Stat. Sol. (a) **201**, 1055 (2004)
- H. Yamane, Y. Yabuuchi, H. Fukagawa, S. Kera, K.K. Okudaira, N. Ueno, J. Appl. Phys. **99**, 093705 (2006)
- C. Tengsted, W. Osikowicz, W.R. Salaneck, I.D. Parker, C.-H. Hsu, M. Fahlman, Appl. Phys. Lett. **88**, 053502 (2006)
- H. Vázquez, Y.J. Dappe, J. Ortega, F. Flores, J. Chem. Phys. **126**, 144703 (2007)
- N. Koch, Chem. Phys. Chem. **8**, 1438 (2007)
- H. Peisert, T. Schwieger, J.M. Auerhammer, M. Knupfer, M.S. Golden, J. Fink, P.R. Bressler, M. Mast, J. Appl. Phys. **90**, 466 (2001)
- A. Hoshino, Y. Takenaka, H. Miyaji, Acta Cryst. B **59**, 393 (2003)
- I. Biswas, H. Peisert, M. Nagel, M.B. Casu, S. Schuppler, P. Nagel, E. Pellegrin, T. Chassé, J. Chem. Phys. **126**, 174704/1-5 (2007)
- H. Peisert, I. Biswas, L. Zhang, M. Knupfer, M. Hanack, D. Dini, M.J. Cook, I. Chambrier, T. Schmidt, D. Batchelor, T. Chassé, Chem. Phys. Lett. **403**, 1 (2005)
- J. Ivanco, B. Winter, T.R. Netzter, M.G. Ramsey, Adv. Mater. **15**, 1812 (2003)
- S. Duhm, G. Heimel, I. Salzmann, H. Glowatzki, R.L. Johnson, A. Vollmer, J.P. Rabe, N. Koch, Nat. Mater. **7**, 326 (2008)
- R. Hesse, T. Chassé, R. Szargan, Anal. Bioanal. Chem. **375**, 856 (2003)

27. A. Gerlach, F. Schreiber, S. Sellner, H. Dosch, I.A. Vartanyants, B.C.C. Cowie, T.-L. Lee, J. Zegenhagen, *Phys. Rev. B* **71**, 205425 (2005)
28. M.P. de Jong, R. Friedlein, S.L. Sorensen, G. Öhrwall, W. Osikowicz, C. Tengsted, S.K.M. Jönsson, M. Fahlman, W.R. Salaneck, *Phys. Rev. B* **72**, 035448 (2005)
29. L. Romaner, G. Heimel, J.-L. Brédas, A. Gerlach, F. Schreiber, R.L. Johnson, J. Zegenhagen, S. Duhm, N. Koch, E. Zojer, *Phys. Rev. Lett.* **99**, 256801 (2007)
30. M.B. Casu, Y. Zou, S. Kera, D. Batchelor, T. Schmidt, E. Umbach, *Phys. Rev. B* **76**, 193311 (2007)